

# Feedbacks between focused melt and localized deformation in the Josephine Peridotite

**AGU  
100**  
ADVANCING EARTH  
AND SPACE SCIENCE



Raphael A. Affinito, Cecile Prigent, Jessica M. Warren

Department of Earth Sciences at the University of Delaware, United States of America

## 1 Introduction

### WHAT:

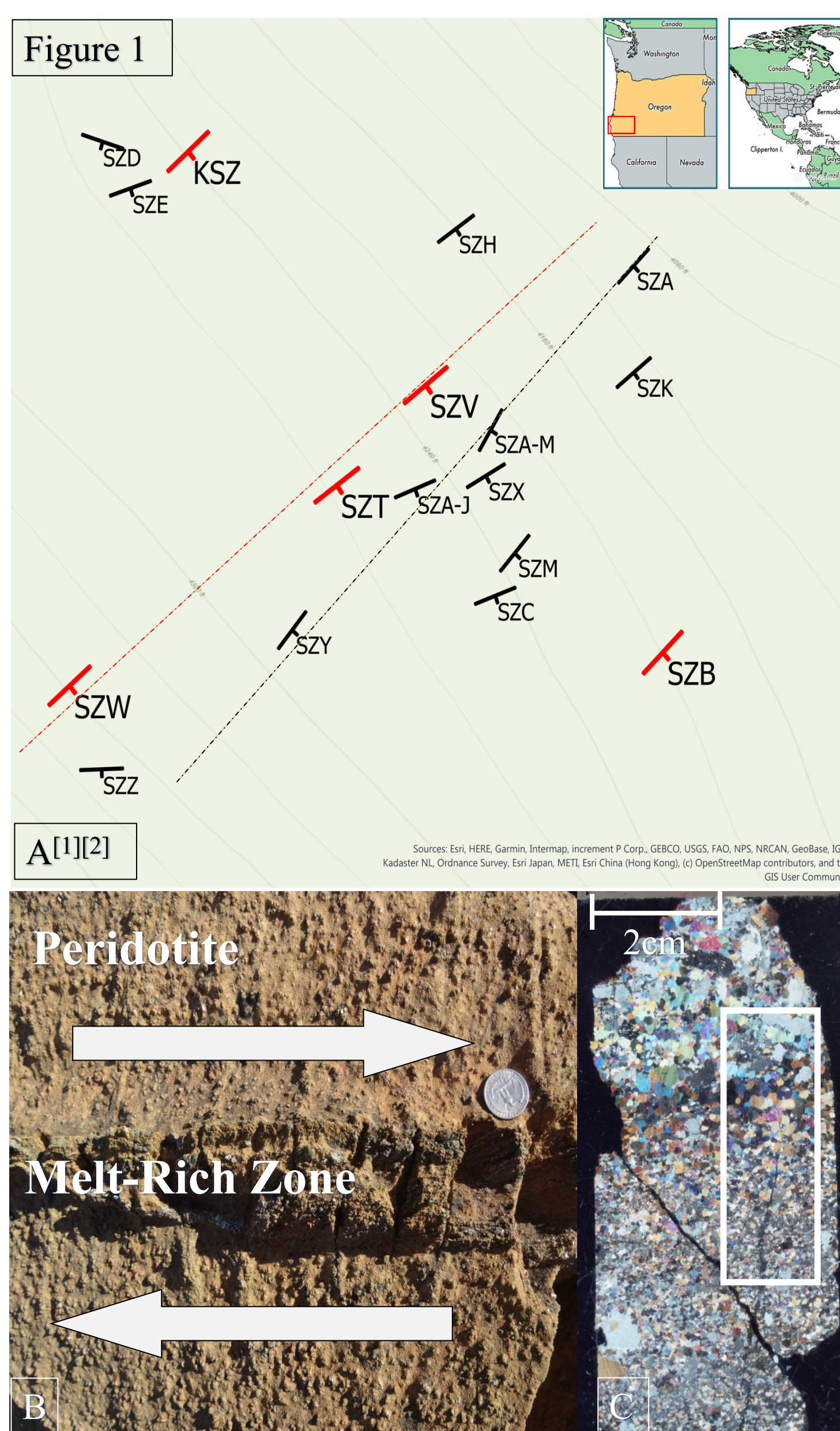
- Understand the interaction between melt percolation and mantle deformation (grain size, texture and deformational mechanisms).
- Explore the scalability and compatibility of experimental and natural results on melt localization processes, along with the influence of melt on mantle seismic anisotropy.

### HOW:

- Comparative analysis of distinct zones within a plagioclase-bearing Peridotite from the Josephine Peridotite.
- Implemented geospatial data, optical analysis and scanning electron microscopy to collect geochemical and microstructural information.

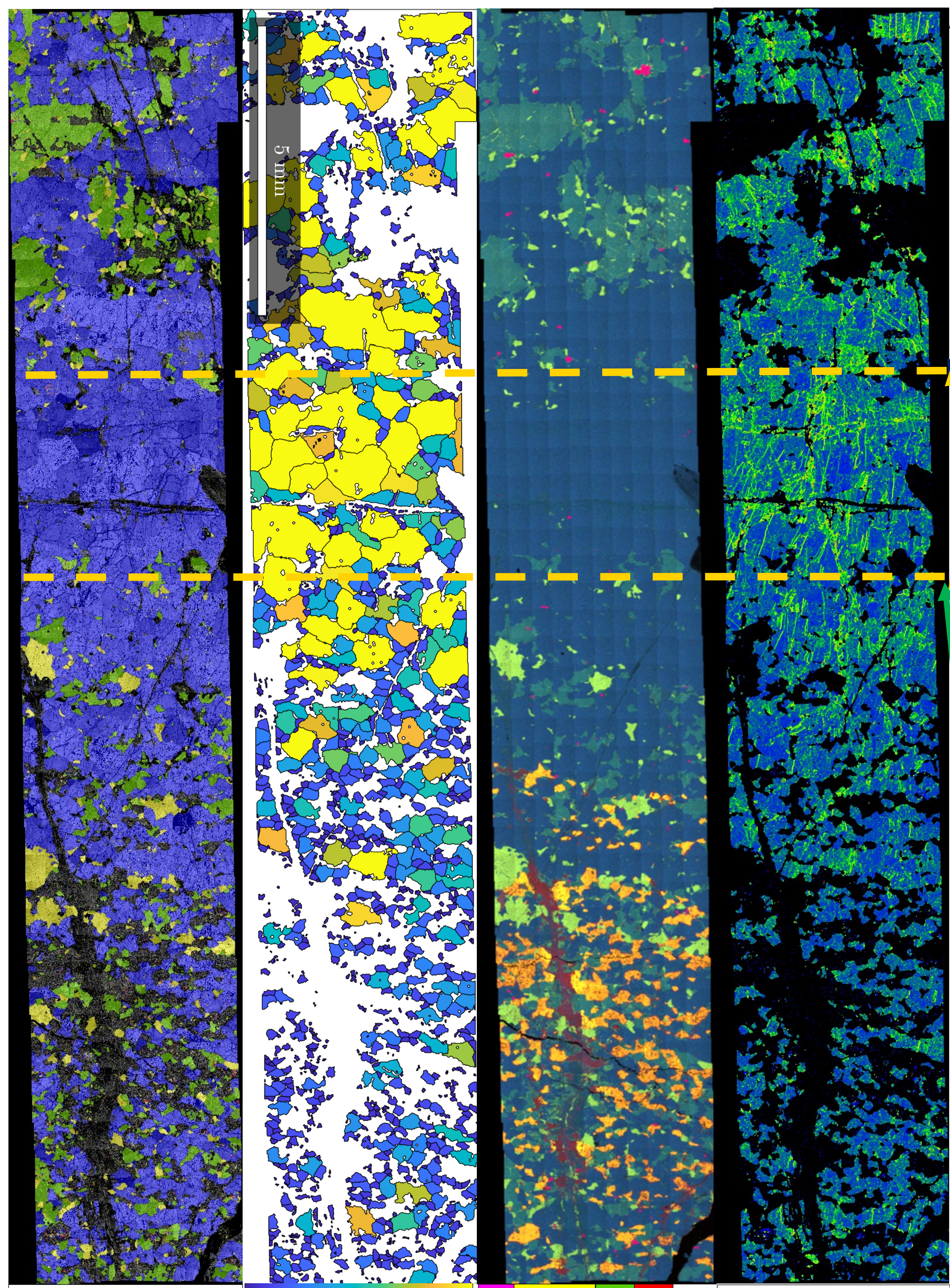
## 2 Geologic Setting

Figure 1



- Figure 1A is a topographic map with contours of 12 meters of the Josephine Peridotite in Southwestern Oregon, U.S.A.
- Denoted by dashed lines is the study area: study adjacent shear zone separated by approximately 30 meters.
- Figure 1B and C are the field sample and thin section respectively. The sample was collected from the red dotted shear zone and point marked SZT.

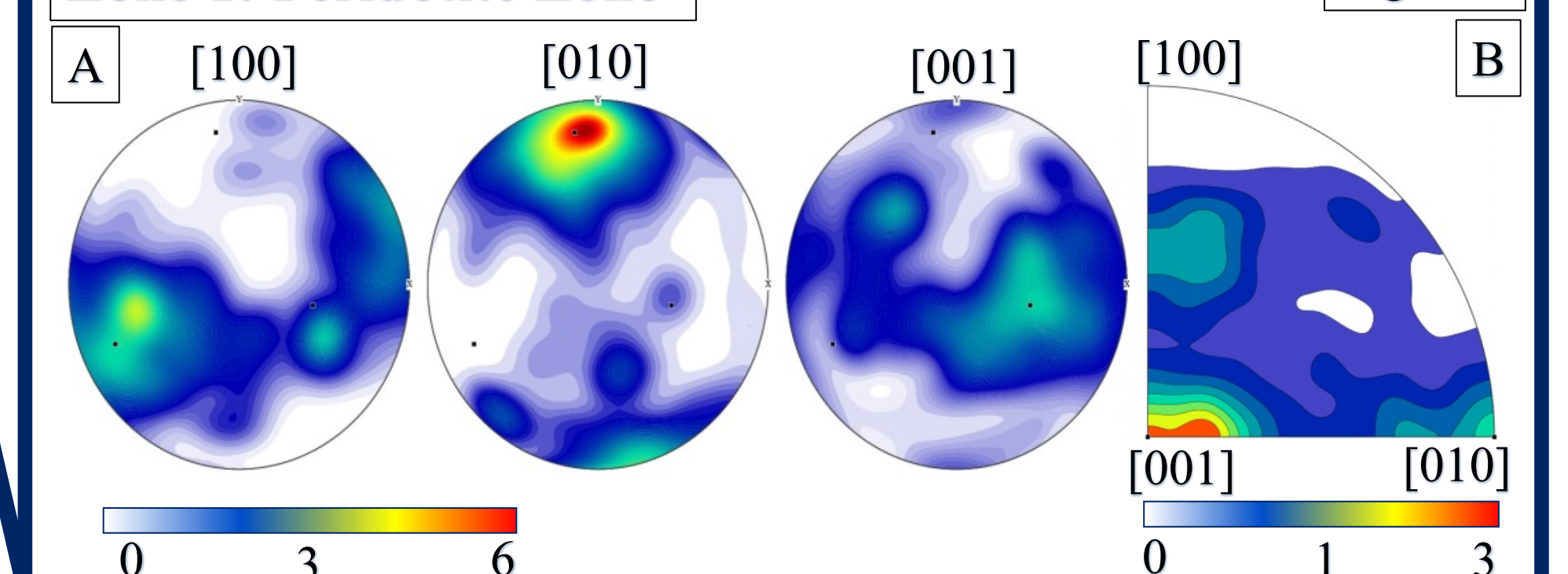
## 3 Data Collection



Figures 2-5 are processed from a large area map collected by the AURIGA 60 SEM in the shared W. M. Keck Center for Advanced Microscopy and Microanalysis (Keck CAMM) at the ISE Laboratory. Figure 2 is a map composed of the band contrast and major components: Olivine (Blue), Clinopyroxene (Yellow) and Orthopyroxene (Green). Figure 3 is a map produced in MATLAB which highlights the olivine grain size. Figure 4 is an EDS map which presents the melt through the plagioclase-clinopyroxene aggregates (Orange). Figure 5 is the Kernel Angle Misorientation of olivine, it shows the sub-grain boundaries and low-angle misorientation intensity.

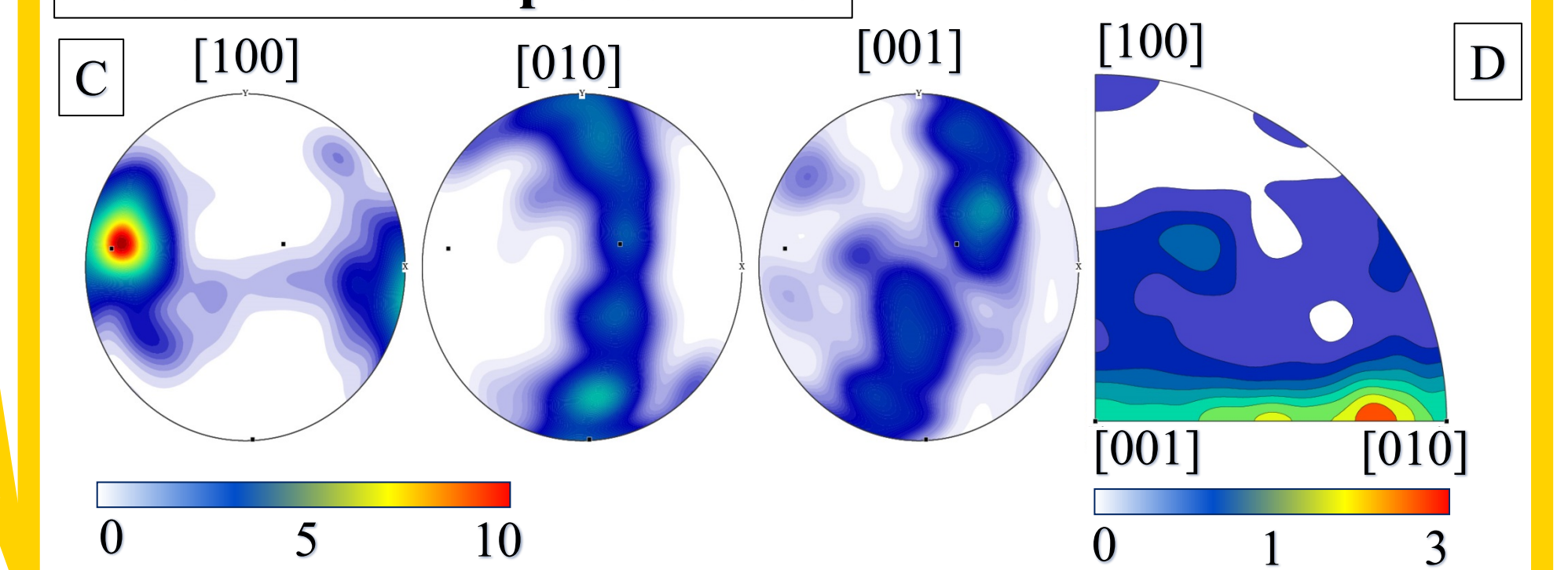
## 4 Structural Results

### Zone 1: Peridotite Zone



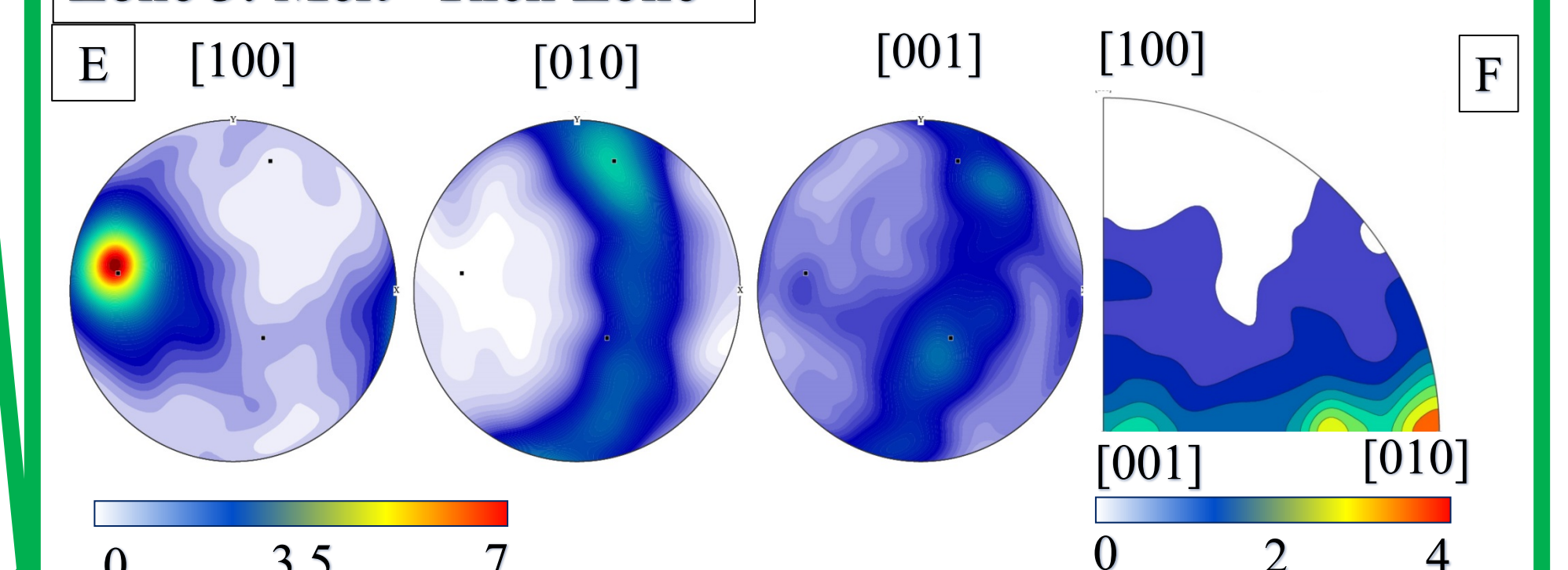
- Olivine is large and euhedral and Orthopyroxene grains are large and has irregular grain shape due to embayment of clinopyroxene and olivine grains.
- There is also the greatest occurrence of spinel in the zone.
- Olivine shows Type A lattice preferred orientation (LPO) and from figure 6B shows rotation of intra-grain misorientation around [001] axis.
- Concentration of LPOs support observations that deformation was accommodated through dislocation creep of olivine along [100](010) slip system.

### Zone 2: Melt - Depleted Zone



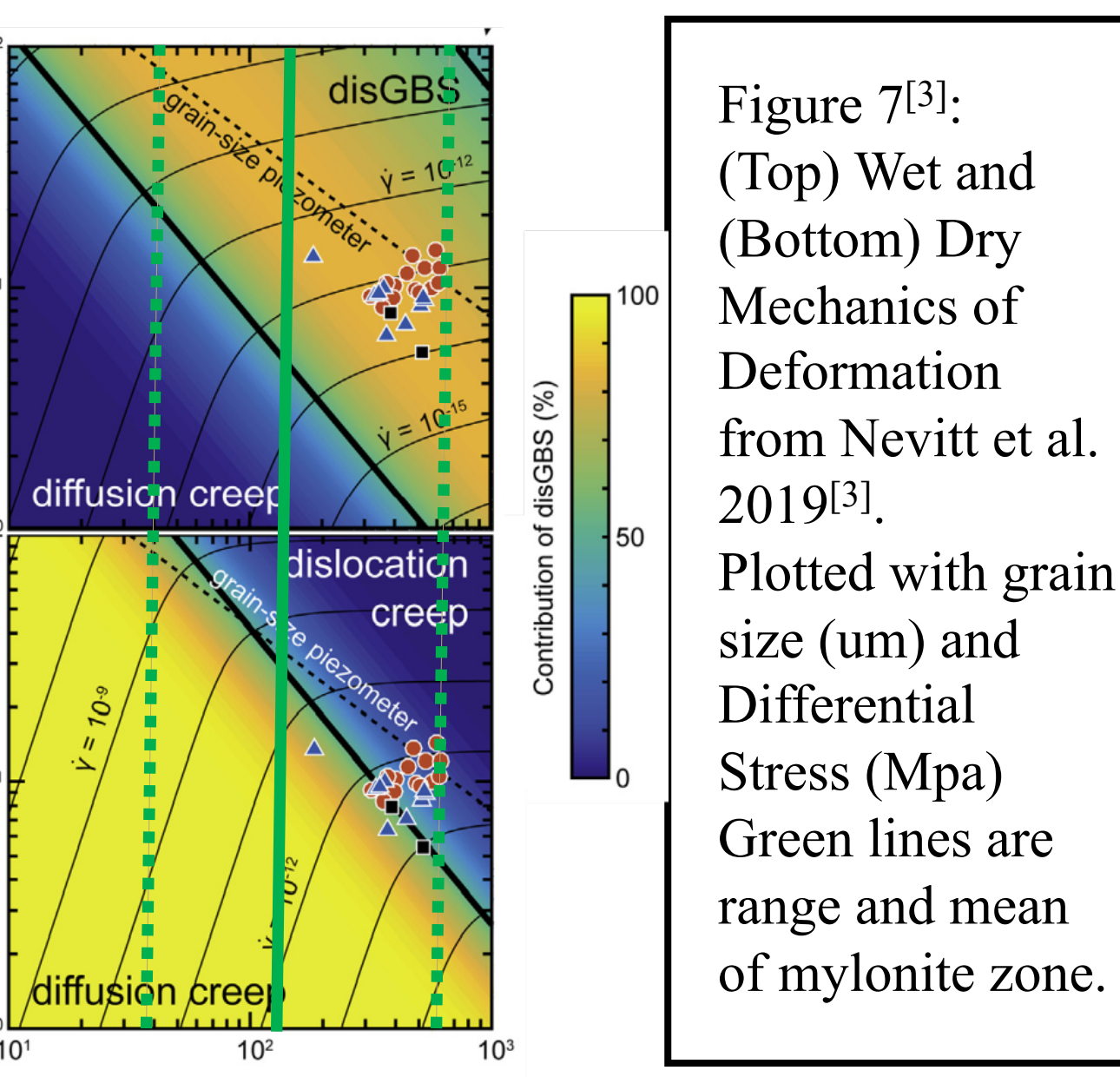
- The larger euhedral olivine grains with triple junctions, evidence of phase equilibrium and recrystallization.
- Absence of melt and the large grain size indicates melt depletion from surrounding zones with limited deformation. Additionally, KAM indicates high density of intragrain misorientation and sub-grain walls in olivine..
- Olivine shows Type D LPO and misorientation maximum around both the [010] and [001] axes. Compared to figures 6a and 6b it indicates that two slip systems were active during deformation.
- Notice that that slip system has migrated and the [010], [001] Euler poles now have a girdle-like concentration.

### Zone 3: Melt - Rich Zone



- Mylonite zone is composed of all major phases and has significant melt presence (Figure 4).
- There is consistent orientation of grains across melt bands.
- Grain size has significantly decreased (Figure 3) and irregular grain shape and embayment of all phases suggest disequilibrium.
- Olivine shows Type D LPO and misorientation maximum around [010], which suggest a change in the dominant system system of dislocation in olivine to the [100](001) slip system in melt-rich zone.

## 5 Discussion



- The three zones show the activation of multiple slip systems in response to melt presence. The presence of melt activates the olivine [100](001) slip system.
- The LPO intensity, characterized by the J-index, increases with increased presence of melt. Strain was localized in melt-rich zone and dominated by dislocation creep (As LPOs are concentrated).
- Grain size reduction and melt presence are linked. We attempted to plot our system onto the flow laws from Nevitt et al 2019. However, more work needs to be done before we can make any statements.

## 6 Conclusion

- Our findings demonstrate that olivine accommodates strain by activating multiple slip systems. It supports the two major slip systems as Type A and D and demonstrates that the activation type may change in response to melt.
- Further studies will need to be conducted comparing samples and accounting for the wet system. Additionally, a larger study would enable resolution for scalability between natural and experimental results.

## 7 References

- Kellemen, Peter B. & Henry J. B. Dick. (1995). "Focused Melt Flow and Localized Deformation in the Upper Mantle: Juxtaposition of Replacive Dunite and Ductile Shear Zones in the Josephine Peridotite, SW Oregon." *Journal of Geophysical Research: Solid Earth*, vol. 100, no. B1, pp. 423–438, doi:10.1029/94jb02063.
- Kumamoto, (2018). *American Geophysical Union, Fall Meeting 2018, abstract #MR41A-01*.
- Nevitt, Johanna M. et al. (2019). "Using geologic structure to constrain constitutive laws not accessible in the laboratory." *Journal of Structural Geology*, vol. 125, pp. 55–63, doi:10.1016/j.jsg.2018.06.006.
- Warren, Jessica M., et al. (2008). "Evolution of Olivine Lattice Preferred Orientation during Simple Shear in the Mantle." *Earth and Planetary Science Letters*, vol. 272, no. 3-4, pp. 501–512, doi:10.1016/j.epsl.2008.03.063.
- Hansen, Lars N. et al. (2014). "Protracted fabric evolution in olivine: Implication for the relationship among strain, crystallographic fabric and seismic anisotropy." *Journal of Earth and Planetary Science Letters*, vol. 387, pp. 157–168, doi.org/10.1016/j.epsl.2013.11.009.
- Karato & Jung (2001). "Effects of water on dynamically recrystallized grain-size of olivine." *Journal of Structural Geology*, vol. 23, pp. 1337–1344, doi.org/10.1016/S0191-8141(01)00005-0